

## Measurements of two-phase flow patterns and local void fraction in vertical rectangular minichannel

ROBERT KANIOWSKI<sup>1\*</sup>  
MIECZYSLAW PONIEWSKI<sup>2</sup>

<sup>1</sup> Kielce University of Technology, al. 1000-lecia Państwa Polskiego 7,  
25-314 Kielce, Poland

<sup>2</sup> Warsaw University of Technology, Plock Campus, Jachowicza 2/4,  
09-402 Plock, Poland

**Abstract** Technology advancements entail a necessity to remove huge amounts of heat produced by today's electronic devices based on highly integrated circuits, major generators of heat. Heat transfer to boiling liquid flowing through narrow minichannels is a modern solution to the problem of heat transfer enhancement. The study was conducted for FC-72 boiling in a rectangular, vertical and asymmetrically heated minichannel that had depths of 0.5–1.5 mm, a width of 20 mm and a length of 360 mm. The heat flux increased and decreased within the range of 58.3–132.0 kW m<sup>-2</sup>, the absolute pressure ranged from 0.116 to 0.184 MPa and the mass flux was 185–1139.2 kg m<sup>-2</sup>s<sup>-1</sup>. The boiling process took place on a flat vertical heating surface made of Haynes-230 0.1 mm thick acid-proof rolled plate with the surface roughness of 121 μm.

**Keywords:** Boiling; Minichannel; Two-phase flow pattern; Void fraction

### Nomenclature

$A$  – area, m<sup>2</sup>  
 $c_p$  – specific heat, Jkg<sup>-1</sup>K<sup>-1</sup>  
 $d$  – diameter, m

---

\*Corresponding Author. E-mail: e-mail kaniowski@tu.kielce.pl

$G$	–	mass flux, $\text{kgm}^{-2}\text{s}^{-1}$
$g$	–	gravity, $\text{ms}^{-2}$
$H$	–	height, m
$h$	–	enthalpy, $\text{Jkg}^{-1}$
$\dot{m}$	–	mass flow rate, $\text{kgs}^{-1}$
$n$	–	number of pixels
$p$	–	pressure, Pa
$\dot{Q}$	–	rate of heat, W
$q$	–	heat flux, $\text{Wm}^{-2}$
$S$	–	velocity ratio
$T$	–	temperature, K
$W$	–	width, m
$X$	–	vapor quality
$x$	–	linear coordinate, m
$y$	–	linear coordinate, m

### Greek symbols

$\alpha$	–	heat transfer coefficient, $\text{Wm}^{-2}\text{K}^{-1}$
$\delta$	–	thickness, m
$\varphi$	–	void fraction
$\lambda$	–	thermal conductivity, $\text{Wm}^{-1}\text{K}^{-1}$
$\mu$	–	viscosity, Pa s
$\rho$	–	density, $\text{kgm}^{-3}$
$\sigma$	–	surface tension, $\text{Nm}^{-1}$

### Subscripts

$F$	–	foil
$f$	–	fluid
$G$	–	glass
$h$	–	hydraulic
$in$	–	inlet
$l$	–	liquid
$m$	–	mean
$sat$	–	saturation
$v$	–	vapor
$w$	–	heating foil

## 1 Introduction

Several consecutive stages take place during boiling. They are related to the vapor void fraction increase in the two-phase mixture as a result of the rise in the heat flux. During the nucleate boiling development, the structure of bubbles changes as a result of the increase in their numbers and volume. In consequence, the slug flow is created, and with further heat supply annular flow is entered (dispersed liquid phase in the vapor core and liquid in

a form of a film on the channel wall) leading to the mist flow. The way the flow structures are shaped depends on pressure, mass flux, hydraulic diameter, and the channel spatial orientation (vertical and horizontal). Therefore the flows are analyzed separately for horizontal channels [1,2] and vertical channels [3,4]. There are significant differences between the mechanisms of vapor bubble nucleation despite apparent similarities. Depending on the channel hydraulic diameter, different two-phase flows are observed for the same channel spatial orientation.

Boiling flow patterns in horizontal channels are similar to the patterns that occur in the vertical channels. At low heat fluxes, gravity may be a major factor in the liquid-vapor distribution asymmetry. In the upper part of the channel adverse heat transfer conditions take a form of a rapid wall temperature rise due to a dryout of the liquid film [5].

The results of the visualization of the subcooled liquid flow in a vertical channel indicate that vapor bubble generation dynamics at the downward flow of the liquid is different from that at the upward flow. If the flow is oriented upwards, vapor bubbles slide along the heating surface and do not depart from it. At the downflow, vapor bubbles depart either immediately after emergence, and then slide along the wall, or slide and then depart from the wall. The process of bubble sliding on the surface causes increased heat transfer between the wall and the liquid, which increases the value of heat transfer coefficient at the flow upwards for the same mass flux and temperature difference [6].

In [7] Thome discussed the issues related to two-phase flow, boiling heat transfer in the flow through minichannels and microchannels, and models for flow boiling in microchannels. He observed that the experimentally obtained flow boiling heat transfer coefficients are closely related to the heat flux and pressure, and slightly dependent on the mass flux and vapor quality. He also found that heat transfer models for conventional channels (macroscale) are not suitable for determining flow boiling heat transfer coefficients in microchannels. The authors of [8] investigated the influence of channel diameter on flow boiling heat transfer in macro- and microchannels. Having compared the heat transfer coefficients obtained by other researchers and solutions for the three-zone model, the authors arrived at the following conclusions: for low values of vapor quality  $X < 0.04$ , the heat transfer coefficient decreases with the increase in diameter; for  $X > 0.18$ , the heat transfer coefficient increases with the increasing diameter; for values  $0.04 > X > 0.18$ , the heat transfer coefficient value rises dramatically

and then falls with the diameter increase.

Bar-Cohen and Rahim in [9] describe a characteristic M-shaped variation of heat transfer coefficient with quality. First maximum value of the coefficient is induced by the transition from bubble to intermittent flow, after which the fall in with increasing quality is caused by the transition into annular flow. Beyond this point the heat transfer coefficient rises until the liquid film evaporates, and then falls rapidly again. The maps of two-phase flow transitions in microchannels for refrigerants and dielectric liquids are also presented in [9] .

It is important to note that numerous theoretical and empirical studies of boiling in minichannels have been conducted in the research centers of Poland [10–14]. The state of the art presented above as well as the literature review shows unequivocally the need for further regular, theoretical and experimental, research of flow boiling heat transfer in minichannels since the effect of thermodynamic parameters on the boiling activity in minichannels with different geometries and spatial orientation has not been clearly determined yet.

The aim of this study is to investigate the complex process of boiling heat transfer in asymmetrically heated minichannels by analyzing the influence of selected thermodynamic parameters and fluid thermal properties on the boiling process and two-phase flow structures/patterns. The flow structures were studied along their evolution path from bubbly flow until the final pattern observed — the mist flow. The problem discussed here has both cognitive and practical aspects in terms of a heat exchanger design.

## 2 Experimental setup

The main loop of the flow system for refrigerant (fluorocarbon) FC-72 consists of the following elements (Fig. 1): the main module (1), rotary pump (2) with a frequency inverter (10) to control the rotational speed of the impeller, tubular heat exchanger (3), rotameter (4), compensating tank (5), recirculation refrigerator (6), filter screen (7), deaerator (8), and a current source (9). Clamps are used to ensure close adherence of the basic module parts.

The measurement module with a minichannel (1) has three measuring tracks, Fig. 2:

- a) color image acquisition with a CCD camera (4), with lighting (4a);

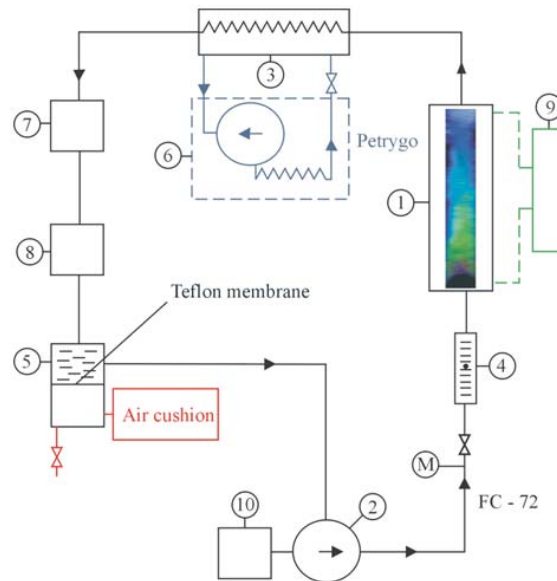


Figure 1. Flow loop: 1 – measurement module; 2 – rotary pump; 3 – tubular heat exchanger; 4 – rotameter; 5 – compensating tank; 6 – refrigerator; 7 – filter; 8 – deaerator; 9 – thyristor converter; 10 – frequency inverter.

- b) two-phase flow pattern acquisition with a monochromatic, high-speed camera; CMOS (5) with lighting (5a),
- c) measurement data acquisition system (3).

On one side of the minichannel, side A, two-dimensional measurement is conducted by means of liquid crystal thermography. On the other side, side B, it is possible to observe two-phase flow structures.

DaqBoard 2000 data acquisition station (3) controlled the acquisition of temperature, pressure and electrical current data. For type K thermocouples the maximum error of temperature measurement was 0.2 K. Pressure measurements at the inlet and outlet were performed to the accuracy of 0.1% of full scale. All the measurement tracks were coupled with the computer (2). The boiling liquid flow rate was read from rotameters. Color image was registered by means of a color video camera, CCD PULNIX TMC 76S, and the image-recording card. The camera was placed perpendicularly to the observed surface covered with a layer of liquid crystals. Lighting was provided by Philips TLD18W/965 fluorescent lamps emitting

white cold light. The distance between the lamps and their positions was adjustable. For the acquisition of flow structures images, the high-speed camera was used, CMOS Photon Focus PHOT MV-D752-160-CL with the resolution of  $752 \times 572$  pixels and frame rate of 347 fps megapixel resolution. Light-emitting diodes were the source of light. The OMEGA water rotameter (4) used in the experiment was rescaled for FC-72. The volume flow rate measurement error in full scale did not exceed 2%.

On one side of the minichannel, two-dimensional measurement is conducted by means of liquid crystal thermography, side A. At the inlet and outlet of the minichannel two thermocouples (type K) and two pressure sensors are mounted. The channel has two surfaces (channel walls) important for the heat exchange process. One of them is the heating surface with the prescribed and constant heat flux, the other one is the glass surface through which the boiling process can be observed, side B.

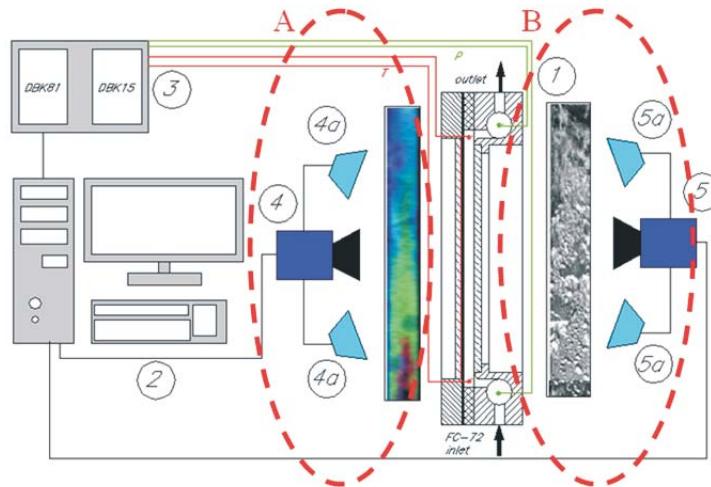


Figure 2. Measurement data acquisition: 1 – measurement module; 2 – computer with frame grabber and monitor; 3 – measurement data acquisition station; 4 – color digital camera, RGB; 4a – lighting emitting white ‘cold’ light; 5 – monochromatic, high-speed digital camera, CMOS; 5a – LED light.

To obtain a good quality photograph of a moving two-phase structure in a long and narrow minichannel, it is necessary to greatly magnify the object being photographed and join two photos into one, Figs. 4 and 5. The photographs of the two-phase structures were taken sequentially, one

after another and one beneath another at a steady state (the same heat flow parameters, camera and light settings, and the same distance from the photographed object). Each digital photo was divided into sets of lines and columns composed of known number of pixels of different colors. A set of pixels contained in one line corresponded to a selected minichannel cross-section, as in Fig. 3.

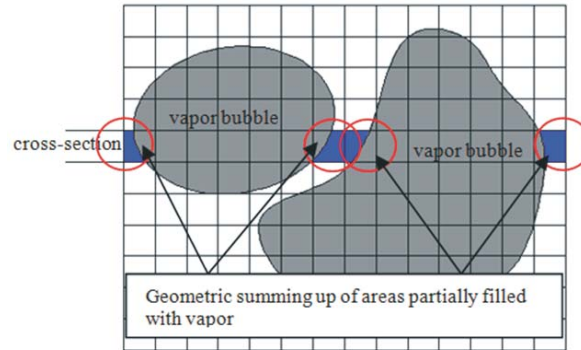


Figure 3. Determining local void fraction  $\varphi$ .

In order to determine void fraction  $\varphi(x)$ , the number of pixels  $n_v$  corresponding to the gas phase in the given line was counted and divided by the total number of pixels  $n$ :

$$\varphi(x) = \frac{n_v}{n}, \quad (1)$$

where  $x$  is the coordinate along minichannel axis, oriented in direction of liquid flow. For the areas partially filled with vapor the procedure of geometrical summing up of all similar areas in the line was used. Because the channel depth was small, 0.5–1.5 mm, bubble curvature in the direction normal to the heating surface was not taken into account.

Void fraction measurements were conducted in four selected cross-sections, Fig. 4, at the distance of 160, 230, 295 and 345 mm from the minichannel inlet. The rulers on both sides of the measurement module with the minichannel facilitated the calibration of the position of the two cameras and positioning of the reference points. The void fraction in one cross-section was determined for 10 consecutive photographs taken at the constant heat flux. The photographs were taken at the speed of 150 fps with the resolution of  $150 \times 752$  pixels.

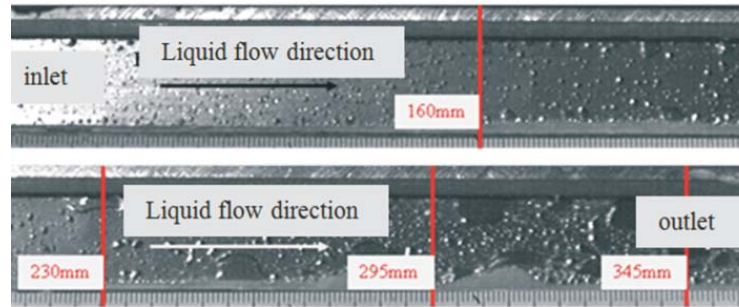


Figure 4. Distribution of cross-sections where void fraction was measured.

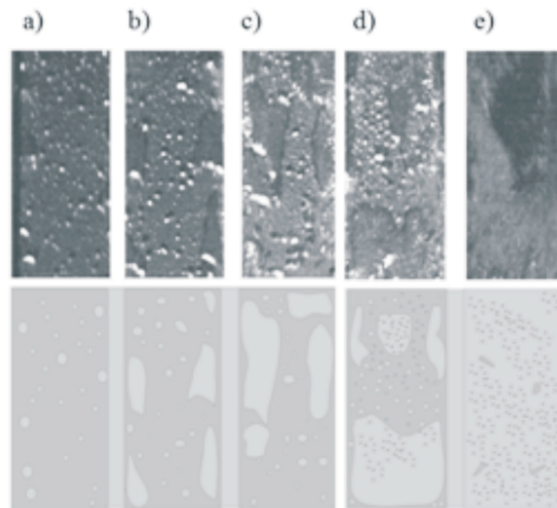


Figure 5. Flow patterns determined in the experiment: a) bubbly flow, b) bubbly-slug flow, c) slug flow, d) wispy-slug flow, e) mist flow.

Flow patterns were determined according to the diagram in Fig. 5: bubbly flow (B) – vapor phase bubbles move in the liquid phase having a spherical shape and small size; larger bubbles are at the minichannel wall; bubbly-slug flow (BS) – bubbles start coalescing to form larger ones at the channel wall; small areas of vapor phase emerge; in the center of the minichannel small spherical bubbles are formed; slug flow (S) – large vapor bubbles separated by liquid phase are generated along the width of the minichannel; wispy-slug flow (WS) – large bubbles coalesce; a small area of vapor with liquid droplets occur in-between; mist flow (M) – liquid phase occurs only

in the form of small droplets. Annular flow pattern was not observed because the minichannel was rectangular, heated on one side and the liquid film on the channel edges dried out. Figure 6 presents typical images of flow patterns at the increase and decrease in the heat flux.

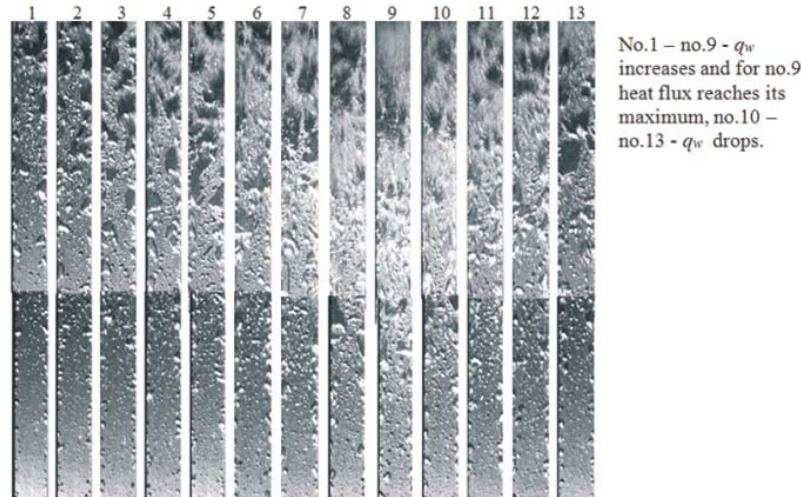


Figure 6. Typical images of flow structures at the increase and decrease of the heat flux,  $d_h = 1.9$  mm,  $p_{in} = 0.119$  MPa,  $G = 569$  kgm<sup>-2</sup>s<sup>-1</sup>,  $q_w = 91.4 - 122.5$  Wm<sup>-2</sup>.

The liquid crystals calibration technique and the method for the heating foil temperature measurement are presented in [15]. The pattern applied for the calculation of the local boiling heat transfer coefficient is shown in Fig. 7. The main elements of the system include FC-72 whose temperature at the inlet to the minichannel is lower than its saturation temperature, and two partitions: the heating foil and the layer of glass. The heating foil with the thermosensitive liquid crystals on its surface is the source of heat. The liquid crystals enable the measurement of the temperature distribution on that surface.

The power supplied to the foil generates the heat flux that is then transferred to the liquid flowing through the minichannel. The element to find is heat transfer coefficient  $\alpha$  on the heating surface cooled with the boiling liquid. This is an inverse problem, in which on the basis of temperature measurement at the internal points of the system (temperature distribution on the heating foil from the side of glass) and measured electrical power supplied to the heater, local heat transfer coefficients are determined for the

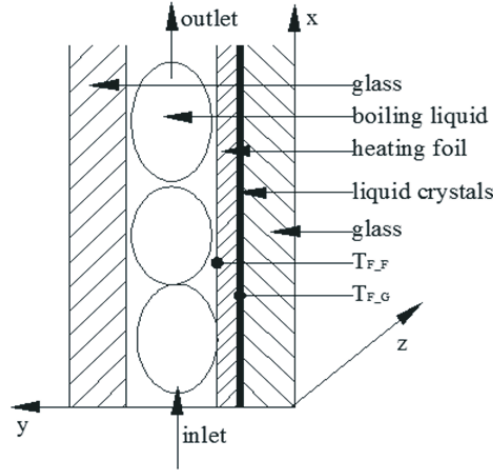


Figure 7. Minichannel cross-section.

internal surface of the heating foil in contact with the liquid. The set elements include: pressure at the minichannel inlet, volumetric flow strength, liquid temperature at the inlet and outlet of the minichannel, and local temperature value of the heating surface over the liquid crystals sensitivity region.

The absolute error did not exceed 5% for local void fraction and 7% for local quality measurement. The measurement error of the heating foil (liquid crystals) temperature reached the highest value 0.76 K. The maximum relative error of the heat flux varied between 0.5 and 3.1%, and that of the local heat transfer coefficient had values in the range of 2.5 to 19.4%. Figure 8 shows typical images of temperature distribution on the heating foil surface at the heat flux increase and decrease.

The presented one-dimensional approach neglects the variability of the heat flux generated inside the foil along coordinate  $x$ , and at the foil-liquid contact type III boundary condition occurs [16]:

$$-\lambda_F \frac{\partial T_F(x)}{\partial y} = \alpha(x) [(T_{F-f}(x) - T_{sat}(x))] = \frac{\dot{Q}}{A_F}. \quad (2)$$

Since the foil is very thin ( $\delta_F \cong 0.1$  mm), the derivative  $\partial T_F / \partial y$  can be replaced with the difference quotient

$$\frac{\partial T_F(x)}{\partial y} = \frac{T_{F-f}(x) - T_{F-G}(x)}{\delta_F}. \quad (3)$$

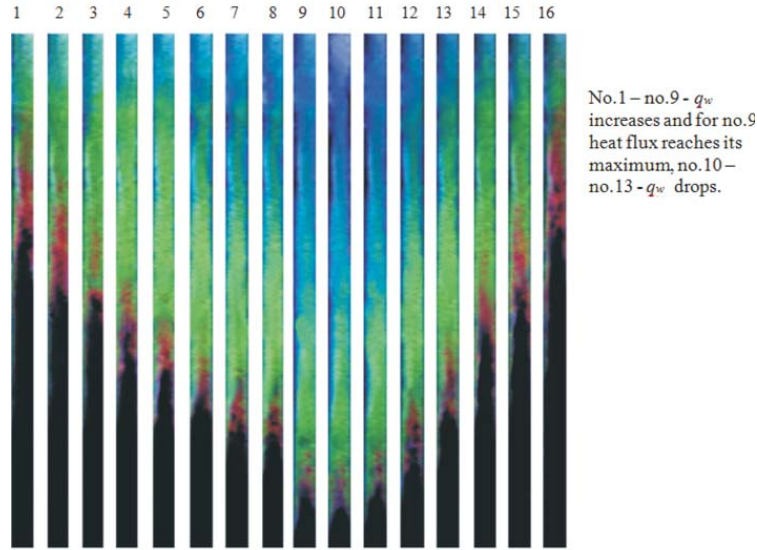


Figure 8. Typical images of temperature distribution on the heating surface at the increase and decrease of the heat flux,  $d_h = 1.9$  mm,  $p_{in} = 0.119$  MPa,  $G = 569$  kgm<sup>-2</sup>s<sup>-1</sup>,  $q_w = 91.4 - 122.5$  Wm<sup>-2</sup>.

From (2) and (3) we obtain the heat transfer coefficient for heat transfer coefficient at the surface of foil-liquid contact:

$$\alpha(x) = \frac{\dot{Q}}{A_F \left( T_{F-G}(x) - \frac{\dot{Q} \delta_F}{A_F \lambda_F} - T_{sat}(x) \right)}. \quad (4)$$

### 3 Results

Visualization of the boiling liquid flow helps understand the mechanism of heat transfer. Ongoing phase change along the whole minichannel length during enhanced boiling makes it impossible to determine clearly the two-phase flow types. Figure 9 depicts images of liquid-vapor flow pattern in a vertical minichannel at the heat flux increase. Two-phase structures were determined to be statistically prevailing in the investigated section. The local void fraction and flow patterns were read for the four cross-sections marked in Fig. 4. The ranges of flow pattern occurrence, depending on the hydraulic diameter,  $d_h$ , and the local void fraction,  $\varphi(x)$ , were the following:

- $d_h = 0.98$  mm: **B** –  $\varphi(x) \leq 0.32$ ; **BS** –  $0.3 \leq \varphi(x) \leq 0.55$ ;  
**S** –  $0.41 \leq \varphi(x) \leq 0.65$ ; **WS** –  $0.5 \leq \varphi(x) \leq 0.9$ ; **M** –  $\varphi(x) \geq 0.9$ ;
- $d_h = 1.9$  mm: **B** –  $\varphi(x) \leq 0.35$ ; **BS** –  $0.24 \leq \varphi(x) \leq 0.5$ ;  
**S** –  $0.34 \leq \varphi(x) \leq 0.7$ ; **WS** –  $0.6 \leq \varphi(x) \leq 0.9$ ; **M** –  $\varphi(x) \geq 0.9$ ;
- $d_h = 2.79$  mm: **B** –  $\varphi(x) \leq 0.6$ ; **BS** –  $0.3 \leq \varphi(x) \leq 0.7$ ;  
**WS** –  $0.65 \leq \varphi(x) \leq 0.9$ ; **M** –  $\varphi(x) \geq 0.9$ .

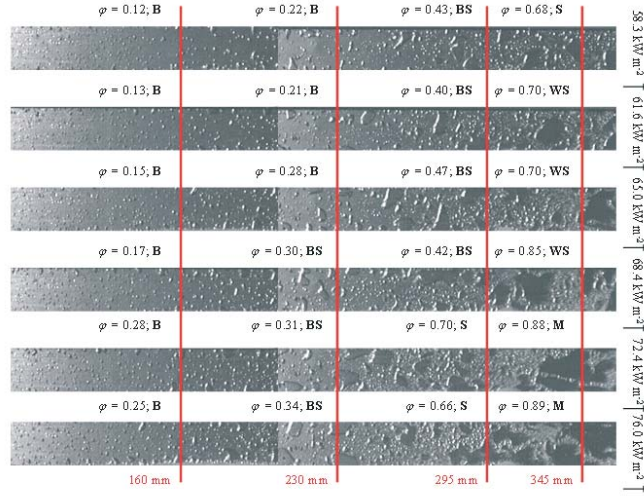


Figure 9. Flow pattern images, sample experiment,  $d_h = 1.9$  mm,  $G = 277$  kgm<sup>-2</sup>s<sup>-1</sup>,  $p_{in} = 0.1196$  MPa, at the increase in the heat flux.

The local thermodynamic vapor quality is given by

$$X(x) = \frac{q_w H(x - x_{sat})}{AGh_{lv}} = \frac{q_w(x - x_{sat})}{WGh_{lv}}, \quad (5)$$

where  $x$  is the distance from the heated section starting point, and  $x_{sat}$  is the location where boiling starts

$$x_{sat} = \frac{\dot{m}\rho_f c_p (T_{sat} - T_{in})}{q_w H}. \quad (6)$$

The local void fraction was determined using several correlations showed below:

Spedding correlation [19]

$$\varphi(x) = \left[ 1 + 2.22 \left( \frac{1 - X(x)}{X(x)} \right)^{0.65} \left( \frac{\rho_v}{\rho_l} \right)^{0.65} \right]^{-1}, \quad (7)$$

Lockhard and Martinelli correlation [18]

$$\varphi(x) = \left[ 1 + 2.28 \left( \frac{1 - X(x)}{X(x)} \right)^{0.64} \left( \frac{\rho_v}{\rho_l} \right)^{0.36} \left( \frac{\mu_l}{\mu_v} \right)^{0.07} \right]^{-1}, \quad (8)$$

Baroczy model [17]

$$\varphi(x) = \left[ 1 + \left( \frac{1 - X(x)}{X(x)} \right)^{0.74} \left( \frac{\rho_v}{\rho_l} \right)^{0.65} \left( \frac{\mu_l}{\mu_v} \right)^{0.13} \right]^{-1}, \quad (9)$$

$$\varphi(x) = \left[ 1 + \left( \frac{1 - X(x)}{X(x)} \right)^{0.64} \left( \frac{\rho_v}{\rho_l} \right) S \right]^{-1}, \quad S = 1 \quad (10)$$

Chihsolm correlation [21]

$$\varphi(x) = \left[ 1 + \left( \frac{1 - X(x)}{X(x)} \right)^{0.64} \left( \frac{\rho_v}{\rho_l} \right) S \right]^{-1}, \quad S = \sqrt{1 - X(x) + \frac{X(x)\rho_l}{\rho_v}}, \quad (11)$$

Steiner correlation [20]

$$\varphi(x) = \frac{X(x)}{\rho_v} \left\{ \left[ 1 + 0.12(1 - X)(x) \left[ \frac{X(x)}{\rho_v} + \frac{1 - X(x)}{\rho_l} \right] + \frac{1.18[1 - X(x)][g\sigma(\rho_l - \rho_v)]^{0.25}}{G\rho_l^{0.5}} \right]^{-1} \right\}. \quad (12)$$

Figure 10 illustrates the relationship between the local void fraction and the local vapor quality when the hydraulic diameter is constant. The comparison of the correlations made by other authors and our experimental results indicates that the correlations fail to satisfactorily describe the relationship between the void fraction and vapor quality in minichannels. The results of the experiments confirm the nature of the investigated phenomenon qualitatively, but they vary from the theoretical values quantitatively.

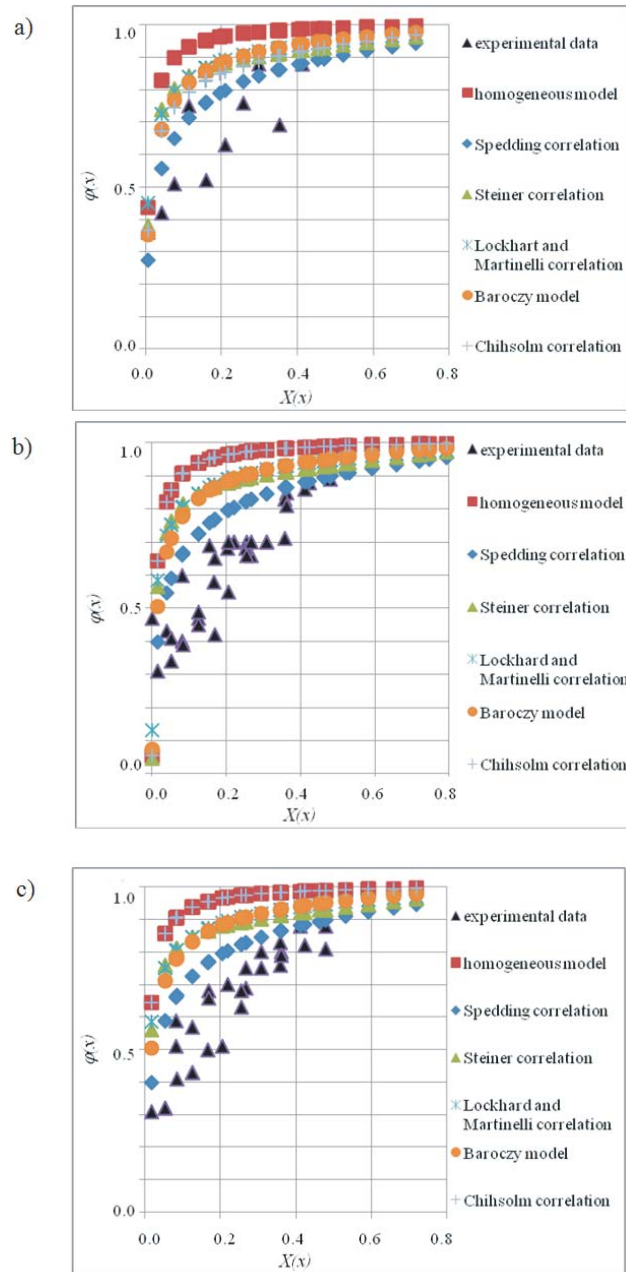


Figure 10. Local void fraction as a function of local vapor quality  $p_{in} = 0.116$  MPa a)  $d_h = 0.98$  mm, b)  $d_h = 1.9$  mm, c)  $d_h = 2.8$  mm.

The review of publications [1,22] shows that at the boiling incipience, the flow boiling heat transfer coefficient increases with the increase in the heat flux. Only in one study, [23], the heat flux had a negligible effect on the coefficient value. The effect of the heat flux on the heat transfer coefficient is presented in Fig. 11a. In our experiment, a clear drop in the local heat transfer coefficient was observed when the heat flux increased during enhanced nucleate boiling, which was due to a substantial increase in the vapor phase. Figure 11b presents sample results for the effect of the liquid pressure at the minichannel inlet on the local heat transfer coefficient at the constant value of the heat flux. Nucleate boiling started at increasing distance from the minichannel inlet since the enthalpy of vaporization increased with pressure. It appeared that when the pressure at the minichannel inlet rose, it caused the rise in the local heat transfer coefficient at the same heat flux values and at the constant mass flux. This agrees with the experimental study results obtained earlier by Lie *et al.* [22]; however, Su *et al.* [24] did not confirm such a relationship.

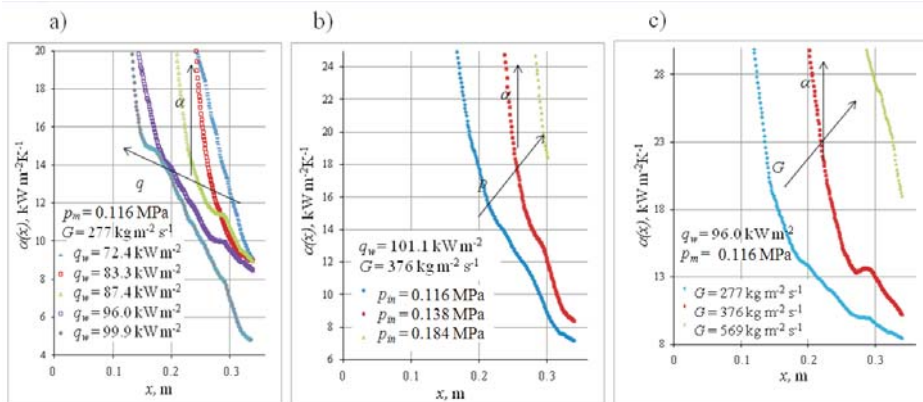


Figure 11. Local heat transfer coefficient as a function of the distance from the minichannel inlet,  $d_h = 1.9$  mm.

Figure 11c summarizes the sample results for the mass flux – local heat transfer coefficient relationship at the constant heat flux. It was found that the local heat transfer coefficient increased along with the increasing mass flux at the same values of heat flux and constant pressure due to the increased Reynolds number. In [1] the boiling heat transfer coefficient was found to be independent of mass flux. The results of one study, [22], reported the coefficient rise with the mass flux increase.

When both the local void fraction and the local vapor quality increase, the local heat transfer coefficient decreases. This is related to the phase change of the working liquid and to the increase in the vapor volume. Experimental data make it possible to read the type of flow pattern at the local void fraction and vapor quality. During the transition from the bubbly-slug to the slug flow, a considerable drop in the heat transfer coefficient is observed.

Figure 12 describes the measurement results for the local heat transfer coefficient as a function of the local void fraction for one measurement. The coefficient decreases with the increase in the local void fraction as a result of the working liquid phase change and the increase in the vapor volume. The experimental data allow reading the flow pattern at the local void fraction. During the transition from the bubble-slug flow into the slug flow pattern, a considerable drop in the heat transfer coefficient is observed.

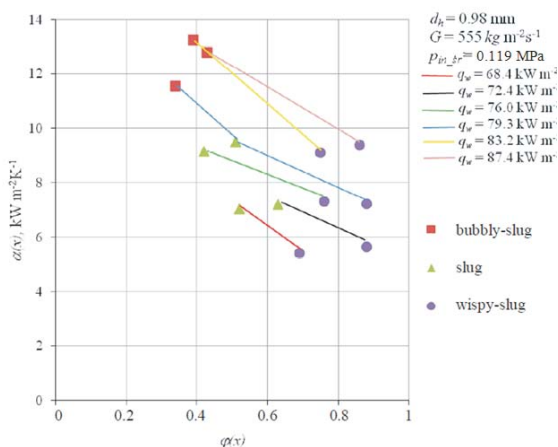


Figure 12. Local heat transfer coefficient as a function of local void fraction.

In the majority of publications analyzed here, the flow boiling heat transfer coefficient decreases with the increase in vapor quality [25], however the authors of [1] do not confirm this finding. Thome *et al.* [26] did not manage to determine ultimately how the subcooling of the boiling liquid to the saturation temperature at the minichannel inlet affects the heat transfer coefficient. The effect of hydraulic diameter on the recorded two-phase flow patterns was not observed either. According to [23,24], the flow boiling heat transfer coefficient increases with the reduced hydraulic diameter of the minichannel, unlike in [27].

## 4 Conclusions

The measurement setup with a high-speed camera made it possible, in the prescribed cross-section, to determine vapor void fractions with relation to the thermal and flow parameters of the boiling liquid at the minichannel inlet. Simultaneous measurements of temperature distribution of the heating surface conducted with thermosensitive liquid crystals made the recorded local void fraction dependent on local temperature. Liquid crystal thermography technique helped to obtain accurate, reproducible measurement of temperature distribution on the heating surface. A possibility to observe the transition field of the heating surface temperature is an advantage of this method.

The following flow types were observed: bubbly, bubbly-slug, slug, wispy-slug and mist flows. The annular flow was not obtained due to technical limitations of the experimental setup (rectangular channel). For similar technical reasons the void fraction for the mist flow was not determined. The ranges of their occurrence, determined only as a function of the local void fraction,  $\varphi(x)$ , overlapped and comprised the following values: bubbly flow –  $\varphi(x) \leq 0.45$ ; bubbly-slug flow –  $0.25 \leq \varphi(x) \leq 0.7$ ; slug flow  $0.3 \leq \varphi(x) \leq 0.74$ ; slug-mist flow –  $0.55 \leq \varphi(x) \leq 0.9$ ; mist flow  $\varphi(x) \geq 0.9$ . The ranges above were disjoint for the fixed minichannel hydraulic diameter  $d_h$ .

Experimental data analysis results indicated that local heat transfer coefficient increased with mass flux and pressure rising at the minichannel inlet. It decreased with the increase in void fraction, vapor quality and heat flux.

**Acknowledgements** This paper was partially supported by the Polish Ministry of Education and Science, Grant No. N N512 477339 (Contract No. 4773/B/T02/2010/39).

*Received 8 March 2013*

## References

- [1] SAISORN S., KAEW-ON J., WONGWISES S.: *Flow pattern and heat transfer characteristics of R-134a refrigerant during flow boiling in a horizontal circular minichannel*. Int. J. Heat Mass Tran. **53**(2010), 4023–4038.

- [2] PIASECKA M., MACIEJEWSKA B.: *The study of boiling heat transfer in vertically and horizontally oriented rectangular minichannels and the solution to the inverse heat transfer problem with the use of the Beck method and Trefftz functions*. Exp. Therm. Fluid Sci., **38**(2012), 19–32.
- [3] KANDLIKAR S.G.: *Scale effects on flow boiling heat transfer in microchannels: A fundamental perspective*. Int. J. Therm. Sci., **49**(2010), 1073–1085.
- [4] ONG C.L., THOME J.R.: *Macro-to-microchannel transition in two-phase flow: Part 1 - Two-phase flow patterns and film thickness measurements*. Exp. Therm. Fluid Sci., **35**(2011), 37–47.
- [5] BOHDAL T.: *Causes of phase change instabilities in heat transferring liquids*. Publishing House of Koszalin University of Technology, Mechanical Engineering, **130**, Koszalin 2006 (in Polish).
- [6] THORNCROFT G.E., KLAUSNER J.F., MEI R.: *An experimental investigation of bubble growth and detachment in vertical upflow and downflow boiling*. Int. J. Heat Mass Tran., **41**(1998), 3857–3871.
- [7] THOME J.R.: *Engineering data book III*. Wolverine Tube Inc. 2004.
- [8] DUPONT V., THOME J.R.: *Evaporation in microchannels. influence of the channel diameter on heat transfer*. In: Proc. 2nd Int. Conf. on Microchannels and Minichannels, Rochester, NY, USA, 2004, 461–468.
- [9] BAR-COHEN A., RAHIM E.: *Modeling and prediction of two-phase microgap channel heat transfer characteristics*. Heat Tran. Eng. **30**(2009), 601–625.
- [10] DUTKOWSKI K.: *Influence of the flashing phenomenon on the boiling curve of refrigerant R-134a in minichannels*. Int. J. Heat Mass Tran. **53**(2010), 1036–1043.
- [11] CIEŚLIŃSKI J., FIUK A.: *Heat transfer characteristics of a two-phase thermosiphon heat exchanger*. Therm. Eng., **51**(2013), 112–118.
- [12] MIKIELEWICZ D., KLUGMANN M., WAJS J.: *Flow boiling intensification in minichannels by means of mechanical flow turbulising*. Int. J. Therm. Sci., **65**(2013), 79–91.
- [13] MIKIELEWICZ D., KLUGMANN M., WAJS J.: *Experimental investigation of M-shape heat transfer coefficient distribution of R123 flow boiling in small-diameter tubes*. Heat Tran. Eng. **33**(2012), 584–595.
- [14] PIASECKA M.: *An investigation into the influence of different parameters on the onset of boiling in minichannels*. Arch. Thermodynam, **33**(2012), 67–90.
- [15] KANIOWSKI R., PONIEWSKI M.E.: *Measurement of void fraction distribution and heating surface local temperature in a rectangular, vertical minichannel heated asymmetrically*. In: Proc. 6th Int. Conf. on Transport Phenomena in Multiphase System — HEAT 2011, 263–270.
- [16] KANIOWSKI R., PONIEWSKI M.E.: *Two-phase flow patterns and boiling heat transfer in asymmetrically heated minichannels*. In: Proc. ECI 8th Int. Conf. on Boiling and Condensation Heat Transfer 2012, CD – paper – o\_s1\_1509.
- [17] SPEDDING P.L., SPENCE D.R.: *Prediction of holdup in two phase flow*. Int. J. Eng. Fluid Mech. **2**(1989), 109–118.

- [18] LOCKHART R.W., MARTINELLI R.C.: *Proposed correlation of data for isothermal two-phase, two-component flow in pipes*. Chem. Eng. Prog., **45**(1949), 39–48.
- [19] BAROCZY C.J.: *Correlation of liquid fraction in two-phase flow with application to liquid metals*. Chem. Eng. Progr. Symp. Ser. **61**(57) (1965), 179–191.
- [20] DALKILIC A.S., LAOHALERTDECHA S., WONGWISES S.: *Effect of void fraction models on the film thickness of R134a during downward condensation in a vertical smooth tube*. Int. Commun. Heat Mass Tran., **36**(2009), 172–179.
- [21] CHISHOLM D.: *Pressure gradients due to friction during the flow of evaporating twophase mixtures in smooth tubes and channels*. Int. J. Heat Mass Tran. **16**(1973), 347–358.
- [22] LIE Y. M., SU F. Q., LAI R. L., LIN T. F.: *Experimental study of evaporation heat transfer characteristics of refrigerants R-134a and R-407C in horizontal small tubes*. Int. J. Heat Mass Tran. **49**(2006), 207–21.
- [23] YANG Y., FUJITA Y.: *Flow boiling heat transfer and flow pattern in rectangular channel of mini-gap*. In: Proc. 2nd Int. Conf. on Microchannels and Minichannels, Rochester, NY, USA 2004, 573–581.
- [24] SU S., HUANG S., WANG X.: *Study of boiling incipience and heat transfer enhancement in forced flow through narrow channels*. Int. J. Multiphas Flow **31**(2005), 253–260.
- [25] HWANG J.W., KIM M. S.: *Two-phase flow heat transfer of R-134a in microtubes*. J. Mech. Sci. Technol. **23**(2009), 3095–3104.
- [26] REVELIN R., THOME J.R.: *Experimental investigation of R-134a and R-245fa two-phase flow in microchannels for different flow conditions*. In: Proc. ECI Int. Conf. Heat Transfer and Fluid Flow in Microscale, Castelvecchio Pascoli, Italy, 2005, CD-No.14.
- [27] TRAN T.N., CHYU M.W., WAMBSGANSS M.W., FRANCE D.M.: *Two-phase pressure drop of refrigerants during flow boiling in small channels: and experimental investigation and correlation development*. Int. J. Multiphas Flow **26**(2000), 1739–1754.